Accurate Carrier Frequency Offset Estimation in Time-Reversal Communications

Chen Chen*†, Hung-Quoc Lai*, Yan Chen*†, and K. J. Ray Liu*†
Origin Wireless Inc., College Park, MD 20742, USA*
ECE Dept., University of Maryland, College Park, MD 20742, USA†
Email: {cc8834, yan, kjrliu}@umd.edu*, quoc.lai@originwireless.net†

***Abstract*—Time-reversal (TR) wideband communication could harvest the energy from the rich-scattering environment and enjoy the unique spatial and temporal focusing effect. However, the performance degrades in the presence of carrier frequency offset (CFO), which introduces an additional phase linear in time. CFO estimators could mitigate its effect. Yet, conventional CFO estimators cannot work well regarding the tiny CFO due to the high sampling rate in wideband TR systems. To address this issue, we propose four CFO estimators which are capable to estimate very small CFO with very high accuracy. Theoretical performance analyses of the proposed estimators are derived. Realizing that phase wrapping could introduce a large bias into estimation, we also derive the condition for phase wrapping avoidance. Extensive experimental results in real environment demonstrate the superiority and applicability of the proposed methods.**

***Index Terms*—Time-reversal wideband communication, carrier frequency offset, phase wrapping, pilot-assisted**

I. Introduction

In wireless communication systems, the local oscillator (LO) at the receiver for down conversion generally runs at a slightly different frequency with that at the transmitter for up conversion [1]. Such frequency misalignment, termed as carrier frequency offset (CFO), introduces an additional phase rotation which increments linearly with time.

By exploiting the redundancy of cyclic prefix in Orthogonal-Frequency-Division-Modulation (OFDM) in time domain, Van De Beek et al. derived the maximum likelihood estimation (MLE) for timing offset and CFO [2]. Schmidl and Cox placed a preamble composed by two identical halves before the data for CFO estimation [3]. The receiver formulated a timing metric as the ratio between the averaged auto-correlation and the energy in one preamble duration. The position of the peak of the timing metric gave a joint estimation of timing offset and CFO estimation. H. Minn et al. [4] and Kim et al. [5] proposed two new preambles in pursuit of sharper timing metrics than the one in [3]. It is shown that the performances of both timing offset estimation and CFO estimation are improved.

Recently, Time-Reversal (TR) wideband communication has gained more and more attentions since it can naturally utilize the multipath in a constructive way [6], [7]. It requires a high bandwidth and thus high sampling rate to capture more resolvable multipath. Moreover, upsampling is generally needed in TR systems to facilitate accurate timing synchronization which makes the sampling rate even higher and leads to a tiny CFO per chip. Directly using the existing CFO estimators may not work well due to the following reasons: (i) The preamble-based methods are impractical since an extremely long preamble is required which significantly degrades the transmission efficiency. (ii) The performance of cyclic prefix based schemes may not be good enough since each cyclic prefix block is different and reusing cyclic prefix blocks is impossible. (iii) Most of existing approaches neglect phase wrapping, which could introduce a bias into estimation [8].

In this paper, we investigate the CFO issue in the TR wideband communication systems and propose methods to counteract it. Using the time-domain pilots, we propose four different CFO estimation methods, i.e., angle-of-mean/mean-of-angle with/without reusing. The main idea is that the phase of the averaged correlation between two adjacent pilot blocks is linear in the CFO. Theoretical analyses are conducted. Impact of phase wrapping on performance is also studied. Finally, real experiments demonstrate the efficiency and effectiveness of the proposed methods.

II. System Model

As shown in Fig. 1, CFO commonly exists in a typical communication system since the LO frequencies at the access point (AP) and the terminal device (TD) cannot perfectly match with each other. For a TR system, due to the asymmetric architecture of the channel probing (CP) phase and data transmission (DT) phase [7], CFO disturbs the two phases differently as follows:

1) In the CP phase, the channel probing signal is transmitted from TD to AP. The estimated channel impulse response (CIR) is affected by CFO, which leads to an inaccurate signature at AP.
2) In the DT phase, the data is convolved with the signature and then transmitted from AP to TD. The effect of CFO is twofold: first of all, the received signal suffers from a time-varying phase shifting due to CFO similar to CP phase. Secondly, the signature which is generated from the estimated CIR is distorted.

A. Signal Model in Channel Probing Phase

In the CP phase, the TD transmits a Golay Pseudorandom Noise (PN) sequence composed by $\{1, -1\}$ with length L_{PN}

978-1-4799-7591-4/15/$31.00 ©2015 IEEE

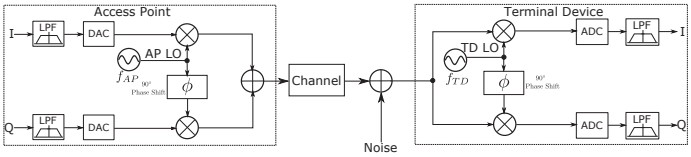

Fig. 1: Carrier Frequency Offset (CFO) in a Typical Communication System

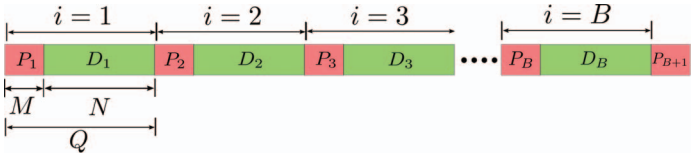

Fig. 2: Data Frame Structure in TR transmission

to the AP which satisfies

$$(G*G)[k] = \sum_{k=0}^{L_{PN}-1} G[m]G[k-m] = L_{PN}\delta[k-(L_{PN}-1)], \tag{1}$$

where δ is the Dirac function, and $*$ the linear convolution.

The received signal at AP is

$$Y_{CP}[k] = (G*h)[k]\exp(j2\pi\Delta f T_s \psi k) + w[k], \tag{2}$$

where $\{h[\ell]\}_{\ell=0,1,\cdots,L-1}$ is the CIR between the AP and the TD, $\Delta f = f_{AP} - f_{TD}$ is the CFO, i.e., the difference between the LO frequencies at the TD and that at the AP, T_s is the baseband sampling interval, ψ is the upsampling ratio, and $w[k] \sim \mathcal{CN}(0,\sigma^2)$.

Then, the CIR can be estimated by convolving the received signal in (2) with the PN sequences as follows

$$\hat{h}[\ell] = \frac{1}{L_{PN}} \sum_{\ell'=0}^{L-1} h[\ell'] \sum_{m=0}^{L_{PN}-1} G[m]G[\ell+L_{PN}-1-\ell'-m] \times e^{j2\pi\Delta f T_s \psi(\ell+L_{PN}-1-m)} + w'[\ell+L_{PN}-1], \tag{3}$$

where $w'[k] = \frac{1}{L_{PN}}(G*w)[k]$ is the average of many zero mean Gaussian noises and thus can be ignored.

Since $\Delta f T_s$ is typically very small for wideband TR systems, $\exp(j2\pi\Delta f T_s\psi(\ell+L_{PN}-1-m))$ can be approximated as $\exp(j2\pi\Delta f T_s\psi(\ell+L_{PN}-1))$ for all m. Then, according to (1), (3) can be rewritten as

$$\hat{h}[\ell] = h[\ell]\exp(j\Delta\omega\psi\ell)\exp(j\theta) + w'[\ell+L_{PN}-1], \tag{4}$$

where $\Delta\omega = 2\pi\Delta f T_s$ is the normalized CFO, and $\theta = 2\pi\Delta f T_s \psi(L_{PN}-1)$ is the common phase error in estimating $\hat{h}[\ell]$.

B. Signal Model in Data Transmission Phase

In the DT phase, the received baseband signal is given by [6]

$$Y[k] = S[k]\exp(-j\Delta\omega D\psi k) + w[k] \tag{5}$$

$$S[k] = (h*g)[L-1]X\left[k-L^\star\right] + \sum_{\substack{l=0,\\ l\neq L^\star}}^{(2L-2)/D} (h*g)[Dl]X[k-l] \tag{6}$$

$$g[k] = \frac{h^*[L-1-k]\exp(-\Delta\omega(L-1-k)\psi)\exp(-j\theta)}{\sqrt{\sum_{\ell=0}^{L-1}|h[\ell]|^2}}, \tag{7}$$

where $L^\star = (L-1)/D$, $X[k]$ is the transmitted symbols, D is the backoff rate, $w[k]$ is the zero-mean complex Gaussian noise with variance σ^2, and $g[k]$ is the signature.

III. Carrier Frequency Offset Estimation

To facilitate CFO estimation, identical pilot symbols are inserted into data blocks. As shown in Fig. 2, the length of one pilot block is M and the length of one data block is N. $Q = M+N$ denotes the length of one transmission block, and i is the block index. One additional pilot block is placed after the last data block. Therefore, there are B data blocks and $B+1$ pilot blocks.

Write the auto-correlation between two adjacent pilot blocks as $\Phi[k,k+Q] = Y[k]Y^*[k+Q], k\in\mathbb{P}$ where $\mathbb{P}$ stands for the index set of pilots, we could estimate the CFO using the estimators given in (8):

$$\widehat{\Delta\omega} = \begin{cases} \frac{\angle\left[\frac{1}{MB}\sum_{i\in\mathbb{B}}\sum_{k\in\mathbb{P}}\Phi[2Qi-2Q+k,2Qi-Q+k]\right]}{Q\psi D}, & \text{AOM-NR} \\ \frac{\sum_{i\in\mathbb{B}}\angle\left[\frac{1}{M}\sum_{k\in\mathbb{P}}\Phi[2Qi-2Q+k,2Qi-Q+k]\right]}{BQ\psi D}, & \text{MOA-NR} \\ \frac{\angle\left[\frac{1}{MB}\sum_{i\in\mathbb{B}'}\sum_{k\in\mathbb{P}}\Phi[Qi-Q+k,Qi+k]\right]}{Q\psi D}, & \text{AOM-R} \\ \frac{\sum_{i\in\mathbb{B}'}\angle\left[\frac{1}{M}\sum_{k\in\mathbb{P}}\Phi[Qi-Q+k,Qi+k]\right]}{BQ\psi D}, & \text{MOA-R} \end{cases} \tag{8}$$

where $\mathbb{B}$ stands for the set $[1,2,\ldots,B]$, $\mathbb{B}'$ for $[1,2,\ldots,B+1]$, AOM for Angle-of-Mean, MOA for Mean-of-Angle, R for reusing, and NR for non-reusing.

IV. Performance Analysis

A. Bias and MSE Performances without Phase Wrapping

To analyze the performance, we make the following assumptions:

Assumption 1: The common phase error $\exp(-j\theta)$ in (5) could be perfectly estimated and compensated.

Assumption 2: Phase wrapping does not occur.

Assumption 3: $S[k]$ has unit power such that $\mathrm{E}\left[|S[k]|^2\right] = 1$.

Assumption 4: $n[k]$ is zero-mean complex Gaussian random variable with equal power of $\sigma^2/2$ on its real and imaginary parts.

Assumption 5: $S[k]$ and $n[k]$ are uncorrelated with each other.

The bias and MSE performances are defined as $\mathrm{Bias}(\widehat{\Delta\omega}) = \mathrm{E}\left[\widehat{\Delta\omega}-\Delta\omega\right]$ and $\mathrm{MSE}(\widehat{\Delta\omega}) = \mathrm{E}\left[(\widehat{\Delta\omega}-\Delta\omega)^2\right]$.

Theorem 4.1: Assuming that AOM-NR and MOA-NR use $2B$ pilot blocks, while AOM-R and MOA-R use $B+1$ pilot blocks. Then, the proposed estimators in (8) are unbiased, i.e.,

$$\mathrm{Bias}(\widehat{\Delta\omega}) = 0, \tag{9}$$

and the MSE performances are given by

$$\mathrm{MSE}(\widehat{\Delta\omega}) = \begin{cases} F\left(\frac{1}{MB}\left[\sigma^2+\frac{\sigma^4}{2}\right]\right), & \text{AOM-NR} \\ F\left(\frac{1}{M}\left[\sigma^2+\frac{\sigma^4}{2}\right]\right)/B, & \text{MOA-NR} \\ F\left(\frac{1}{MB}\left[\frac{\sigma^2}{B}+\frac{\sigma^4}{2}\right]\right), & \text{AOM-R} \\ V(M,\sigma^2), & \text{MOA-R} \end{cases} \quad (10)$$

where $F(x), V(x,y), U(x,y)$ are shown as follows.

$$F(x) = \frac{\int_0^{\frac{\pi}{2}} \frac{2y^2}{\sqrt{2\pi x}} \exp\left(-\frac{\tan^2(y)}{2x}\right) \frac{1}{\cos^2(y)} dy}{Q^2\psi^2 D^2}, \quad (11)$$

$$V(x,y) = \frac{G(y)}{B} + \frac{2(B-1)}{B^2Q^2\psi^2D^2}U(x,y), \quad (12)$$

$$U(x,y) = \int_{u=-\infty}^{\infty}\int_{v=-\infty}^{\infty} \arctan(u)\arctan(v) \frac{x}{2\pi\left(y+\frac{y^2}{2}\right)\sqrt{1-\frac{1}{(2+y)^2}}} \exp\left(-\frac{\left[\frac{x\left(u^2+v^2+\frac{2uv}{2+y}\right)}{y+\frac{y^2}{2}}\right]}{2\left(1-\frac{1}{(2+y)^2}\right)}\right) dudv. \quad (13)$$

B. Bias and MSE Performances with Phase Wrapping

The results in Theorem 4.1 are derived without phase wrapping. In case of phase wrapping, we must modify the performances as follows:

Theorem 4.2: When phase wrapping occurs, the bias and MSE of the proposed estimators should be modified as

$$\mathrm{Bias}(\widehat{\Delta\omega'}) = \pm\frac{2k\pi}{Q\psi D}, k \in \mathbb{Z}, k \neq 0, \quad (14)$$

$$\mathrm{MSE}(\widehat{\Delta\omega'}) = \mathrm{MSE}(\widehat{\Delta\omega}) + \frac{4k^2\pi^2}{Q^2\psi^2D^2}, k \in \mathbb{Z}, k \neq 0, \quad (15)$$

where $\widehat{\Delta\omega'}$ is the estimated CFO with phase wrapping, and $\mathbb{Z}$ stands for the set of integers.

C. Limitation on Distance between Adjacent Pilot Blocks

Larger Q could improve the performance shown by (11) and (12). However, it might trigger the phase wrapping issue which introduces a bias into estimation.

Firstly, consider the noiseless case, where $\Phi[k, k+Q] = |S[k]|^2\exp(j\Delta\omega Q\psi D), k \in \mathbb{P}$ when $w[k] = 0$. If $|\Delta\omega Q\psi D| < \pi$, $\Delta\omega$ can be perfectly estimated using (8). However, when $|\Delta\omega Q\psi D| > \pi$, the estimation $\widehat{\Delta\omega'}$ is biased by $\frac{2k\pi}{Q\psi D}$ shown by (14). Thus, we should ensure $|\Delta\omega Q\psi D| < \pi$. Secondly, for noisy case, to increase the robustness in presence of noise, the condition is modified as

$$Q < \lambda Q^+ = \frac{\lambda\pi}{|\Delta\omega|D\psi}, \lambda \in (0,1] \quad (16)$$

Parameter	Notation	Value
Data Block Length	N	128
Pilot Block Length	M	32
Transmission Block Length	Q	160
# of Frames	B	88
Back-off Rate	D	4
Oversampling Ratio	ψ	4
Sampling Frequency	f_s	125MHz
Sampling Interval	T_s	8ns
Carrier Frequency	f_c	5.8GHz
Combining Factor	W	$[2, 4, 6, 8, 16]$
# of Trials	U	500

TABLE I: Configuration of Parameters in Experiment

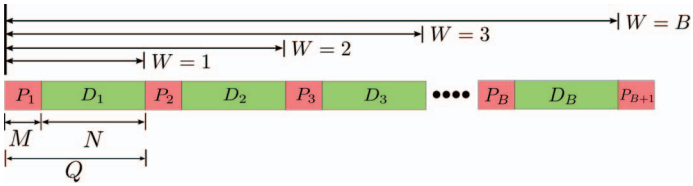

Fig. 3: Frame Structure in Experiments

V. Experimental Results

To test the performance of our CFO methods, we use our TR boards for experiments [9]. First, we perform the over-the-cable (OTC) tests by connecting the TR transmitter and receiver via a cable with 50 dB attenuation with 24 dB transmitting power. Then, we conduct the over-the-air (OTA) tests by antennas with 27 dB transmitting power. The parameter settings are summarized into Table I.

Despite the fixed Q and B settings, we could emulate the effects of different Q and B by putting adjacent transmission blocks together, which is described in Fig. 3. By tuning the combining factor W, we could achieve different effective Q values, given by $Q_{\text{eff}}(W) = WN+(W-1)M$. Given that the total length of data is calculated as $N \times B$ excluding the last pilot block, by choosing different W and thus different Q_{eff}, we should tune the effective number of data blocks as well, given as $B_{\text{eff}}(W) = \left\lfloor \frac{NB}{WN+(W-1)M} \right\rfloor$, and $B_{\text{eff}}(W)$ is further rounded into the nearest odd number. Such flexibility enables us to obtain performances using different pilot separations with the same experimental results. For notational convenience, we omit the argument W in $Q_{\text{eff}}(W)$ and $B_{\text{eff}}(W)$.

In practice, it is very hard to know the ground-truth CFO. Thus, for performance evaluation, we turn to the Error-Vector-Magnitude (EVM). It is defined as $\mathrm{EVM}[\hat{\mathbf{X}}] = \frac{1}{|\mathcal{U}|}\sum_{i\in\mathcal{U}} 20\log_{10}||\mathbf{X}^i_{\text{orig}} - \hat{\mathbf{X}}^i||_2$ where $\hat{\mathbf{X}}$ is the vectorized restored data symbols after CFO compensation, $\mathbf{X}_{\text{orig}}$ the known transmitted data, $||\mathbf{x}||_2$ the $\mathcal{L}2$ norm of vector $\mathbf{x}$, and $\mathcal{U}$ the index subset out of the 500 frames after eliminating outliers.

In Fig. 4(a), we demonstrate the estimated CFO using AOM-R scheme in one of our OTA tests. $Q_{\text{eff}} \in [288, 608, 1248, 1888, 2528]$, and $M = 32$. B_{eff} scales with Q_{eff} accordingly. For fairness, we use the first $\frac{B_{\text{eff}}+1}{2}$ pilot blocks for reusing schemes, and all B_{eff} pilot blocks for non-

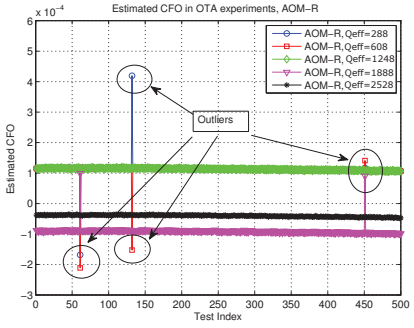

(a)

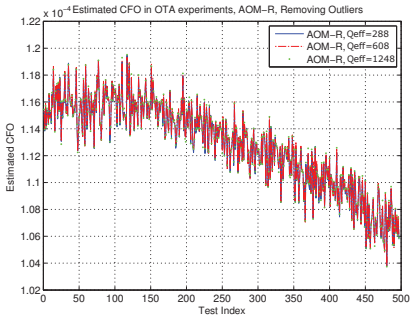

(b)

Fig. 4: Experimental Results of AOM-R estimator, OTA Test, Basic Signature: (a) with Outliers (b) Without Outliers.

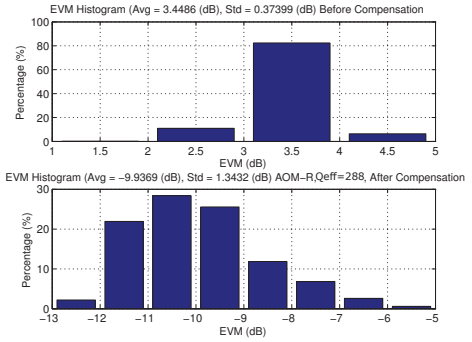

(a)

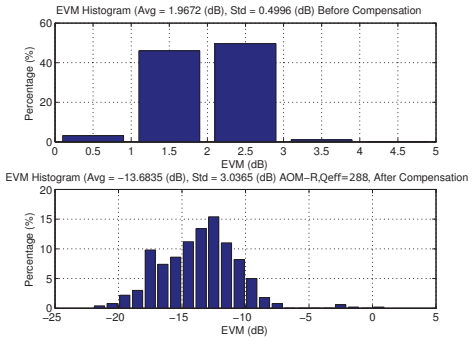

(b)

Fig. 5: Effect of CFO Compensation on EVM: (a) OTA (b) OTC.

reusing schemes. We can observe that (i) The estimated CFO is time-varying instead of static. (ii) In few experiments, the estimated CFO is unreasonably large. This might be due to the bursty board noise and other non-idealities in our TR boards. (iii) For the cases of $Q_{\text{eff}} = 1888$ and 2528, the estimated CFO is significantly different from the results of $Q_{\text{eff}} = 288, 608, 1248$ since (16) is violated.

Fig. 4(b) illustrates the results after dropping the outliers for each Q_{eff} and the phase wrapping cases. As we can see, the estimated CFO only changes in a very small range, implying the stability of the proposed estimators.

In Fig. 5(a), we draw the histogram of EVM performances before and after CFO compensation. It can be clearly seen that CFO compensation is necessary as it improves the EVM performance from 3.45dB to -9.93dB when $Q_{\text{eff}} = 288$. We tabulate the averaged EVM in dB scale into Table II with scaling Q_{eff} and B_{eff}. The improvement of reusing against non-reusing is denoted by $\Delta(\text{AOM})$ and $\Delta(\text{MOA})$ respectively. The results imply that increasing Q_{eff} does not necessarily improve the performance, since the effect is balanced off by the decrease of B_{eff} and the CFO may change slowly with time.

The improvement of EVM after CFO compensation is shown in Fig. 5(b), and the results of EVM performances are summarized into Table III. The EVM for OTC is much better than the OTA case since the channel is very close to line-of-sight (LOS) with only one significant tap, and the variance of channel noise is smaller.

W	Q_{eff}	B_{eff}	AOM-R	AOM-NR	$\Delta(\text{AOM})$
2	288	39	-9.94	-9.72	0.22
4	608	19	-9.95	-9.56	0.39
8	1248	9	-9.95	-9.89	0.06
W	Q_{eff}	B_{eff}	MOA-R	MOA-NR	$\Delta(\text{MOA})$
2	288	39	-9.94	-9.72	0.22
4	608	19	-9.97	-9.59	0.38
8	1248	9	-9.97	-9.92	0.05

TABLE II: Performance of OTA

W	Q_{eff}	B_{eff}	AOM-R	AOM-NR	$\Delta(\text{AOM})$
2	288	39	-13.68	-13.31	0.37
4	608	19	-13.70	-13.25	0.45
8	1248	9	-13.71	-13.66	0.05
W	Q_{eff}	B_{eff}	MOA-R	MOA-NR	$\Delta(\text{MOA})$
2	288	39	-13.72	-13.35	0.37
4	608	19	-13.72	-13.27	0.45
8	1248	9	-13.72	-13.68	0.04

TABLE III: Performance of OTC

VI. Conclusion

In this paper, we propose four highly accurate schemes to estimate the tiny CFO for time-reversal systems with assistance from time-domain pilots. Effect of CFO is analyzed for both the channel probing and data transmission phases. Theoretical analyses are rigorously derived together with the conditions to avoid phase wrapping. Extensive experimental results in real environment validate the superiority of the proposed schemes.

REFERENCES

[1] T.-D. Chiueh and P.-Y. Tsai, *OFDM Baseband Receiver Design for Wireless Communications*. John Wiley and Sons (Asia) Pte Ltd, 2007.

[2] J. van de Beek, M. Sandell, and P. Borjesson, "ML estimation of time and frequency offset in OFDM systems," *IEEE Trans. Signal Processing*, vol. 45, pp. 1800 –1805, jul 1997.

[3] T. Schmidl and D. Cox, "Robust frequency and timing synchronization for OFDM," *Communications, IEEE Transactions on*, vol. 45, pp. 1613–1621, Dec 1997.

[4] H. Minn, M. Zeng, and V. Bhargava, "On timing offset estimation for OFDM systems," *Communications Letters, IEEE*, vol. 4, pp. 242–244, July 2000.

[5] J. Kim, J. Noh, and K. Chang, "Robust timing frequency synchronization techniques for OFDM-FDMA systems," in *Signal Processing Systems Design and Implementation, 2005. IEEE Workshop on*, pp. 716–719, Nov 2005.

[6] B. Wang, Y. Wu, F. Han, Y.-H. Yang, and K. J. R. Liu, "Green wireless communications: A time-reversal paradigm," *Selected Areas in Communications, IEEE Journal on*, vol. 29, pp. 1698–1710, September 2011.

[7] Y. Chen, F. Han, Y.-H. Yang, H. Ma, Y. Han, C. Jiang, H.-Q. Lai, D. Claffey, Z. Safar, and K. J. R. Liu, "Time-reversal wireless paradigm for green Internet of Things: An overview," *Internet of Things Journal, IEEE*, vol. 1, pp. 81–98, Feb 2014.

[8] C. Chen, Y. Chen, N. Ding, Y. Wang, J.-C. Lin, X. Zeng, and D. Huang, "Accurate sampling timing acquisition for baseband OFDM power-line communication in Non-Gaussian noise," *Communications, IEEE Transactions on*, vol. 61, pp. 1608–1620, April 2013.

[9] Z. Wu, Y. Han, Y. Chen, and K. J. R. Liu, "A time-reversal paradigm for indoor positioning system," *Vehicular Technology, IEEE Transactions on*, vol. PP, no. 99, pp. 1–1, 2015.